Polymer Chemistry

RSCPublishing

ARTICLE

Electronic Supporting Information for: Exploiting an end group functionalization for the design of antifouling bioactive brushes

A. R. Kuzmyn,[a] A. de los Santos Pereira,[a] O. Pop-Georgievski,[a] M. Bruns,[b] E. Brynda[a] and C. Rodriguez-Emmenegger [a,]*

[a] Institute of Macromolecular Chemistry, Academy of Sciences of the Czech Republic, v.v.i., Heyrovsky sq. 2, 162 06 Prague, Czech Republic. E-mail: rodriguez@imc.cas.cz

[b] Institute for Applied Materials and Karlsruhe Nano Micro Facility (KNMF), Karlsruhe Institute of Technology (KIT), 76344 Eggenstein-Leopoldshafen, Germany.

* To whom all correspondence should be addressed: Dr. Cesar Rodriguez-Emmenegger, rodriguez@imc.cas.cz (rodriguez@imc.cas.cz)

Additional methods used for the physicochemical characterization of the surfaces

Spectroscopic ellipsometry

The thickness of the polymer brushes in the dry state was determined by ellipsometry using a Variable Angle Spectroscopic Imaging Auto-Nulling Ellipsometer EP3-SE (Nanofilm Technologies GmbH, Germany) in the wavelength range of λ = 399–811 nm (source Xe-arc lamp, wavelength step ~10 nm) at an angle of incidence AOI = 70º in air at room temperature. The thickness and refractive index of polymer layers were obtained from simultaneous fitting of the measured ellipsometric data using Cauchy dispersion function ($n = A_n + B_n/\lambda$, $k = 0$ with $A_n = 1.452 \pm 0.014$, $B_n = 5900 \pm 100$ [nm^2] for poly(MeOEGMA).

Water Contact Angle

The dynamic water contact angles were measured with a contact angle goniometer OCA 20 (DataPhysics Instruments, Germany) equipped with SCA 20 software. A 5 μL water drop was deposited on tested surfaces, and dynamic changes of the drop profiles were recorded on 5 μL advancing and receding volumes at a flow rate of 0.1 $\mu L \cdot s^{-1}$. The profiles were fitted with the tangent leaning method. Reported values are averages of four measurements recorded at different positions on each substrate.

Atomic Force Microscopy

All images were acquired with a Multimode Atomic Force Microscope NanoScope IIIa (Digital Instruments) as topological scans in tapping mode in air, using silicon probes OTESPA (Veeco Instruments) with a nominal spring constant of 42 $N \cdot m^{-1}$ and a tip radius of 7–10 nm. Areas of 5 × 5 μm^2 (512 × 512 pixels) were scanned at a rate of 1 Hz. The scans were analyzed using Gwyddion software.

FTIR Grazing Angle Specular Reflectance (FTIR-GASR)

FTIR Grazing Angle Specular Reflectance spectroscopy (GASR) of the dry coatings on gold-coated SPR chips was performed using a Nexus 870 FTIR spectrometer equipped with a Smart SAGA GASR attachment (ThermoFisher Scientific). For each sample, 512 scans were taken at a resolution of 4 cm^{-1} with an aperture size of 16 mm.

Results

Characterization of the polymer brushes before and after Cp-substitution

The polymerization kinetics were monitored by following the increase in thickness of the layers with polymerization time (Figure S1). The linear growth confirms a well-controlled polymerization. The formation of a hydrophilic polymer layer is supported by the dynamic water contact angles (Table S1). The thickness of the polymer brushes remains essentially unchanged after the substitution of the bromine end-groups with cyclopentadiene (Cp). This substitution is accompanied by a rearrangement of the hydrophobic-hydrophilic balance in the topmost layer of the polymer brush, as seen by the increase in the advancing contact angle of the Cp-modified polymer brushes.

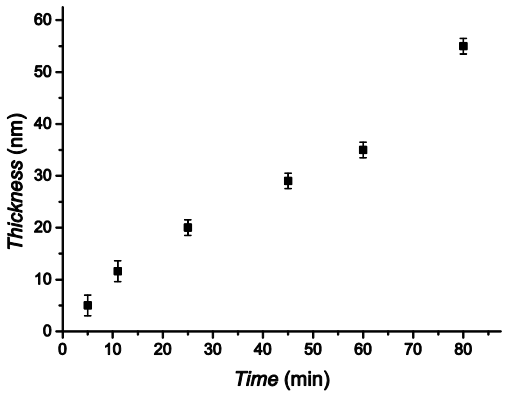

Fig. S1 Evolution of poly(MeOEGMA) brushes dry thickness with polymerization time. The dry thickness of the polymer layers was determined by spectroscopic ellipsometry.

Table S1 Thickness and dynamic water contact angles before and after Cp substitution of the bromine end-group on the poly(MeOEGMA) brushes.

Surface	Thickness [nm]	Contact angle [°]	
		Advancing	Receding
Poly(MeOEGMA)-Br	11.6 ± 0.5	41.2 ± 0.7	29.4 ± 1.2
Poly(MeOEGMA)-Cp	10.1 ± 1.0	50.4 ± 0.8	27.3 ± 1.0
Poly(MeOEGMA)-Br	20.4 ± 0.6	42.2 ± 0.7	25.0 ± 0.5
Poly(MeOEGMA)-Cp	19.0 ± 0.9	48.1 ± 1.5	25.3 ± 1.3
Poly(MeOEGMA)-Br	28.7 ± 0.5	43.6 ± 0.6	23.8 ± 0.4
Poly(MeOEGMA)-Cp	29.0 ± 0.3	52.3 ± 1.1	21.8 ± 0.6

Representative FTIR-GASR spectra of the poly(MeOEGMA) brushes terminated in Br and Cp are shown in Figure S2. In the C-H region the polymer brushes showed characteristic bands of CH_2 and CH_3 stretching modes of the oligo(ethylene glycol) methyl ether side chains and the aliphatic main chain. In the region below 1800 cm^{-1} the spectra exhibited a strong peak at 1730 cm^{-1} arising from the ester carbonyl and a family of bands having their origin in CH_2 scissoring (~ 1465 cm^{-1}), wagging (~ 1350 cm^{-1}), twisting (~ 1250 cm^{-1}), and rocking (~ 950 cm^{-1}) modes. The strongest band in the spectra is observed at 1145 cm^{-1} and can be assigned to the C-O-C stretching modes of the OEG subunits. The spectra confirm that the chemical structure of the poly(MeOEGMA) brush is not changed during the substitution of the bromine end-group with Cp. Additionally, in the region of 1650–1550 cm^{-1} which is free of the polymer brush contributions, the presence of Cp gives rise to the weakly pronounced band at 1600 cm^{-1} which can be attributed to C=C stretching ring vibrations. The other expected characteristic bands are buried under the dominating contributions of the polymer brush.

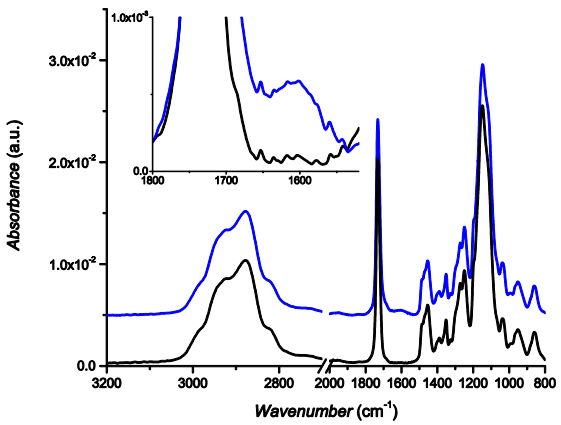

Fig. S2 FTIR-GASR spectra of poly(MeOEGMA)-Br (1) and of poly(MeOEGMA)-Cp (2) with thickness of about 30 nm. The insert presents the overlapped spectra in the region free of the polymer brush contributions. The presence of CP gives rise to the band at 1600 cm^{-1} which can be attributed to C=C stretching ring vibrations.

Ex situ immobilization of α-maleimide-ω-methoxy-(polyethylene glycol) on Cp-modified SAMs

In order to further confirm the successful substitution of the bromine groups by Cp, the end-group modification reaction was preformed directly on a self-assembled monolayer of ω-mercaptoundecyl bromoisobutyrate (SAM-Br) and the surfaces (Scheme S1) were examined by XPS (Figure S3) and ToF-SIMS (see Figure 1 of the main article). The spectra show the complete disappearance of the bromine peaks after the substitution.

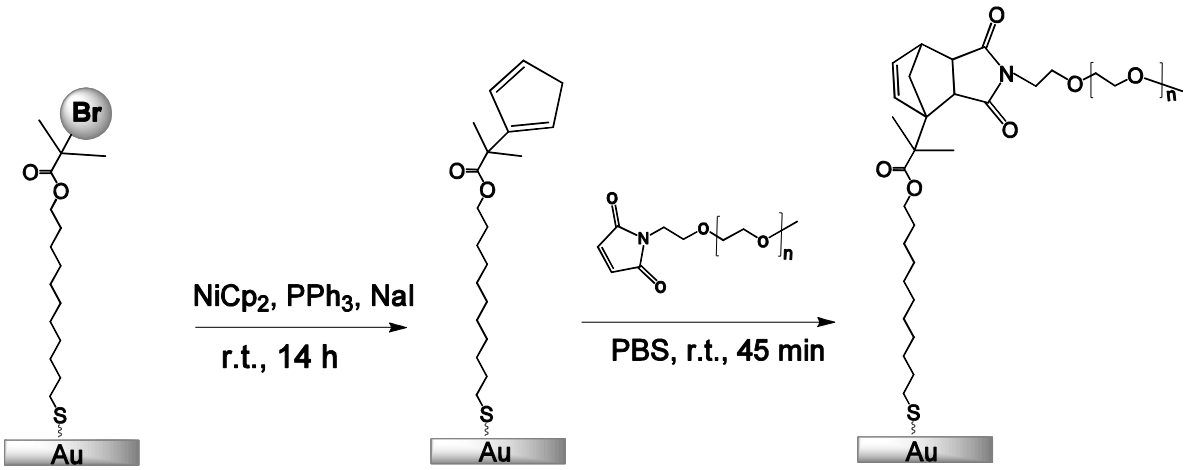

Scheme S1 Cp-substitution of bromine end-group the SAM and immobilization of α-maleimide-ω-methoxy-(polyethylene glycol) on the resulting SAM-Cp. The procedure employed was the same as for poly(MeOEGMA)-Br brushes.

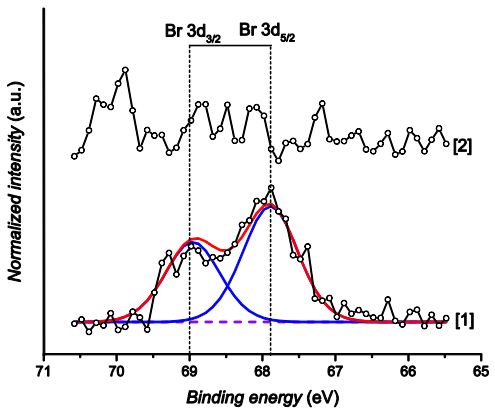

Fig. S3 XPS spectra SAM-Br (1) and SAM-Cp (2).

To further verify the Cp-substitution on the SAM and its reactivity, the immobilization of α-maleimide-ω-methoxy-(polyethylene glycol) (PEG-M) was performed on SAM-Cp. The SAM-Cp surfaces were covered with a solution of 1 mg·mL^{-1} PEG-M in PBS and kept in a chamber saturated with water vapor at room temperature for 45 min. The chips were then rinsed with copious amounts of deionized water and ethanol, and dried by blowing nitrogen, after which XPS (Figure S4) and FTIR-GASR (Figure S5) spectra were recorded. An analogous experiment was performed on the same type of surface using PEG not functionalized with maleimide for control purposes.

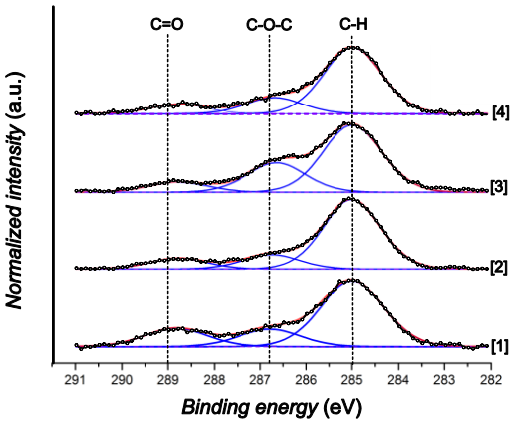

Fig. S4 XPS spectra SAM-Br [1], SAM-Cp [2], SAM-Cp-M-PEG [3], and control SAM-Cp after PEG not functionalized with maleimide [4].

Figure S5 summarizes the FTIR spectra obtained for the substitution reactions of the bromine end-group by Cp, and the immobilization of PEG-M to the activated SAM-Cp surfaces.

In the CH stretching region, the spectrum of SAM-Br is dominated by vibrations at 2980, 2920 and 2852 cm^{-1} arising from the asymmetric and symmetric CH_3 and CH_2 stretching vibrations of the ω-mercaptoundecyl bromoisobutyrate chains. Below 1800 cm^{-1} the spectrum shows a distinctive C=O stretching band of the ester bond at 1730 cm^{-1}, symmetric CH_2 and asymmetric CH_3 bending bands at 1465 cm^{-1}, C-O stretching bands at 1278 and 1110 cm^{-1}, and a dominating skeletal vibration band at 1175 arising from the C-$(CH_3)_2$ structure.

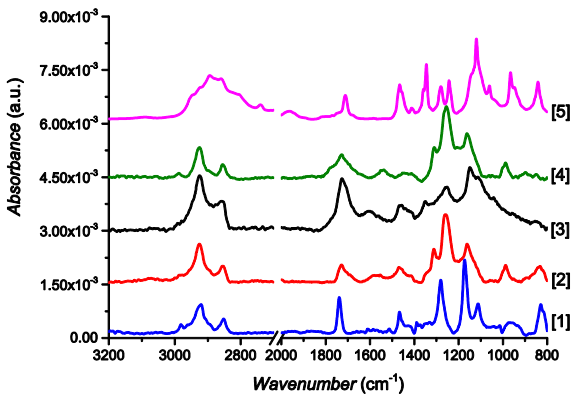

Fig. S5 Representative FTIR-GASR spectra of SAM-Br [1], SAM-Cp [2], SAM-Cp-M-PEG [3], control SAM-Cp after exposure PEG not functionalized with maleimide [4]. The reference M-PEO [5] spectrum is reported for comparison.

The substitution of the bromine end-group by Cp causes significant changes in the originally measured spectrum of SAM-Br. The spectrum of SAM-Cp is characterized by a significant broadening of the C=O band. Additionally, the presence of Cp (C=C stretching) gives the rise to a weak and broad band at about 1600 cm^{-1}, and family of bands at 1570, 1310, 1257, 1160 cm^{-1} characteristic for the C-H bending vibrations of the cyclopentadienyl ring.[1, 2] Interestingly, despite these significant changes, in the CH stretching region the presence of Cp gave rise to very weak bands (at about 3073 cm^{-1}) arising from the =C-H modes.

The successful immobilization of PEG-M to the activated SAM-Cp surfaces is evidenced by the significant increase in the intensity of the asymmetric and symmetric CH_2 bands (at 2920 and 2852 cm^{-1}), the C=O stretching band of the ester bond at 1730 cm^{-1}, and the two strong C-O-C stretching bands of the EG monomer units at 1147 and 1117 cm^{-1}.[3, 4] This findings by FTIR-GASR are corroborated by the XPS spectra in the C 1s region, which an increase in intensity for the C-O-C envelope at 286.8 eV. It is important to note that the control spectra of SAM-Cp exposed to non-reactive PEG completely lacked any spectral features of PEG. This further verified the specificity of the cyclopentadiene-maleimide Diels-Alder ligation and the presence of Cp at the distal-end of the SAM.

Confirmation of the specificity of the attachment of BSA-M

Additional SPR experiments were carried out to prove that the attachment of maleimide-conjugated proteins to the poly(MeOEGMA) brushes presenting Cp groups was exclusively due to the maleimide-Cp click reaction. On a non-Cp-modified brush (poly(MeOEGMA)-Br), a solution of 1 $mg \cdot mL^{-1}$ BSA-M in PBS was injected for 45 min (Figure S6). The sensogram shows that no attachment occurred, as λ_{res} returns to the original baseline after contact.

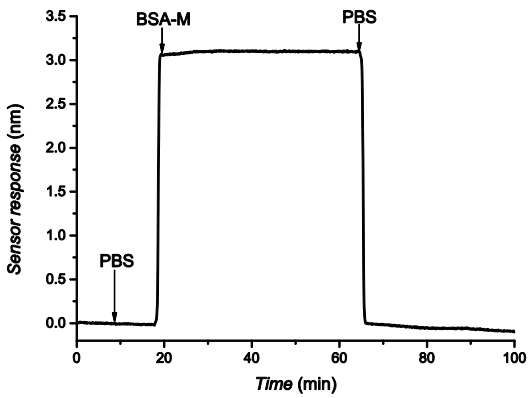

Fig. S6 SPR sensogram of contact of BSA-M with a poly(MeOEGMA)-Br surface of 10 nm thickness.

Stability of Cp-modified Poly(MeOEGMA) Brushes

To assess the stability of the Cp-modified brushes BSA-M was clicked on poly(MeOEGMA)-Cp of 10 nm thickness, which was stored for 6 months in deionized water at 4 ºC after the Cp substitution. The attachment of BSA-M was performed following the same procedure presented in the experimental section and measured in real time by SPR (Figure S7). Specific conjugation of BSA-M was observed; while no adsorption of non-modified BSA occurred, confirming the stability of the Cp groups in the polymer brush.

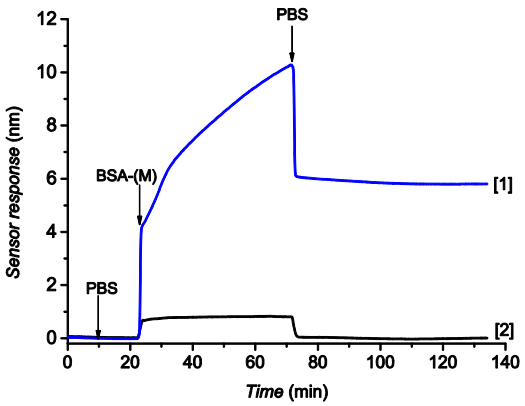

Fig. S7 SPR sensogram showing the attachment of BSA-M (1) and non-modified BSA (2) on a surface of poly(MeOEGMA)-Cp with thickness of 10 nm, after storage in water for 6 months.

Fouling from blood plasma

Non-specific adsorption of undiluted human blood plasma (BP) was assessed in real time by SPR. Table S2 presents the fouling after 15 min exposure to BP.

Table S2. Fouling from undiluted blood plasma

Surface	Fouling from Blood Plasma [pg·mm^{-2}]
Au	3000 ± 400
Poly(MeOEGMA)-Br (10 nm)	170 ± 38
Poly(MeOEGMA)-Cp (10 nm)	192 ± 28
Poly(MeOEGMA)-Cp-BSA-Anti-BSA (10 nm)	207 ± 45
Poly(MeOEGMA)-Br (20 nm)	160 ± 23
Poly(MeOEGMA)-Cp (20 nm)	150 ± 15
Poly(MeOEGMA)-Cp-BSA-Anti-BSA (20 nm)	81 ± 45
Poly(MeOEGMA)-Br (30 nm)	120 ± 15
Poly(MeOEGMA)-Cp (30 nm)	105 ± 15
Poly(MeOEGMA)-Cp-BSA-Anti-BSA (30 nm)	87.5 ± 64

AFM Topography of the Surfaces

The AFM topography images (Figure S8) show homogeneous morphology and low roughness of the SAM and poly(MeOEGMA) brushes, which are preserved after the Cp-substitution of the bromine end-groups. The morphology of the brushes after conjugation of BSA-M suggests the formation of a nascent layer that could be attributed to attached protein.

Au (R_q = 1.4 ± 0.1 nm)

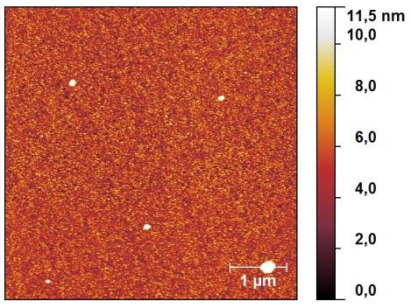

SAM-Br (R_q = 1.8 ± 0.1 nm)

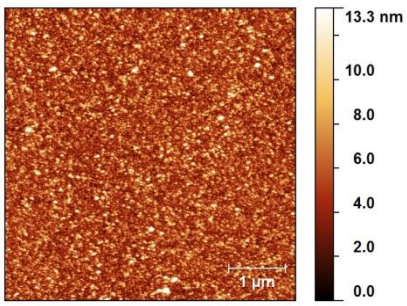

SAM-Cp (R_q = 1.5 ± 0.1 nm)

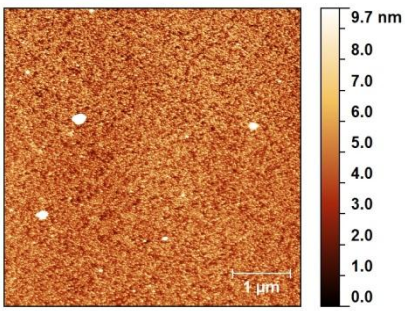

Poly(MeOEGMA)-Br (R_q = 1.0 ± 0.6 nm)

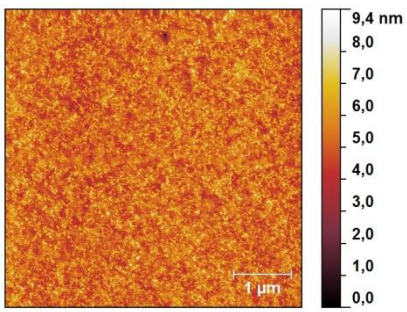

Poly(MeOEGMA)-Cp (R_q = 1.6 ± 0.2 nm)

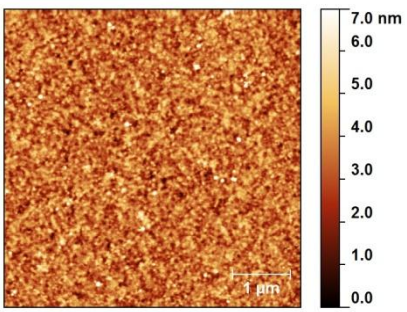

SAM-Cp-M-PEG (R_q = 2.2 ± 0.2 nm)

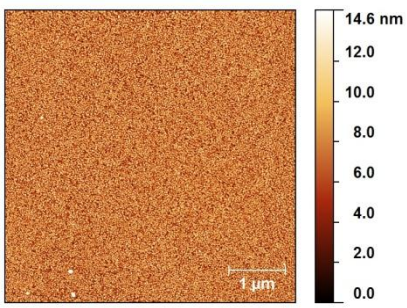

Poly(MeOEGMA)-Cp-M-BSA (R_q = 1.9 ± 0.4 nm)

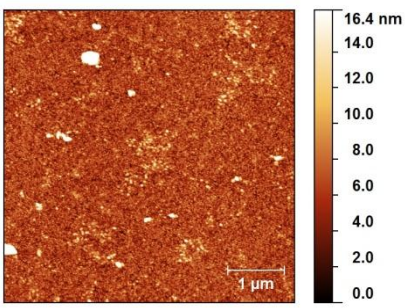

Fig. S8 Representative AFM topography images of the obtained surfaces after each modification step. The root-mean-square roughness (Rq) is also reported.

Verification of the absence of Ni by XPS

No appreciable amount of Ni could be detected by XPS. The survey spectra of poly(MeOEGMA) and SAM samples after the substitution of end-groups with Cp show no peaks at 854.4, 871.7, and 1008.4 eV, the expected binding energies of Ni $2p_{3/2}$, Ni $2p_{1/2}$, and Ni 2s, respectively.[5]

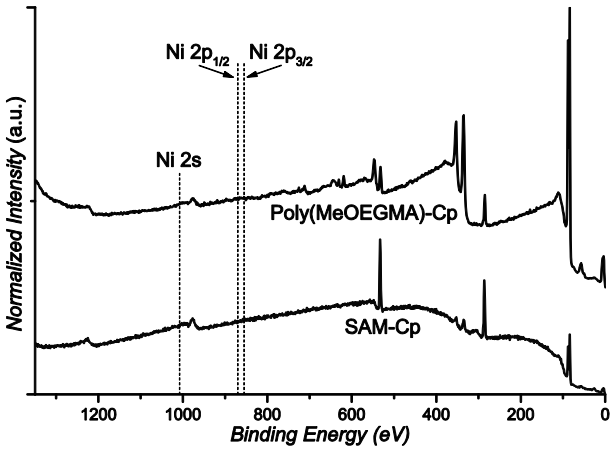

Fig. S9 XPS survey spectra of poly(MeOEGMA) and SAM surfaces after Cp substitution.

Confirmation of the attachment of BSA-M to Cp-modified brushes by FTIR-GASR

The successful introduction of cyclopentadiene groups and their conjunction with M-BSA can be further confirmed by independent FTIR-GASR measurements. In the region of 1800 − 1500 cm^{-1}, the IR spectrum of poly(MeOEGMA)-Cp conjugated with M-BSA is characterized by additional bands at 1640 and 1520 cm^{-1} (Figure S10).

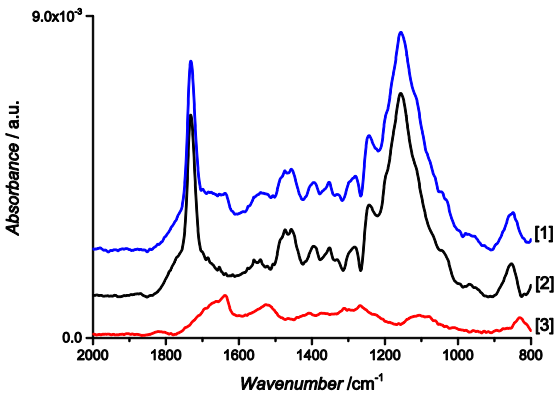

Fig. S10 FTIR-GASR spectra of BSA-M clicked to poly(MeOEGMA)-Cp (1) and of poly(MeOEGMA)-Cp (2) polymer brushes with thickness of about 10 nm. Their differential spectrum (3) is reported for comparison. The successful conjugation of BSA-M to the polymer brushes can be confirmed by the amide bands at 1640 and 1520 cm^{-1}.

References

1. S. F. Tayyari, S. Laleh, M. Zahedi-Tabrizi and M. Vakili, *J. Mol. Struct.*, 2013, **1038**, 177-187.
2. S. F. Tayyari, S. Laleh, M. Zahedi-Tabrizi and M. Vakili, *J. Mol. Struct.*, 2013, **1036**, 151-160.
3. O. Pop-Georgievski, S. Popelka, M. Houska, D. Chvostova, V. Proks and F. Rypacek, *Biomacromolecules*, 2011, **12**, 3232-3242.
4. O. Pop-Georgievski, D. Verreault, M. O. Diesner, V. Proks, S. Heissler, F. Rypáček and P. Koelsch, *Langmuir*, 2012, **28**, 14273-14283.
5. C. A. Tolman, W. M. Riggs, W. J. Linn, C. M. King and R. C. Wendt, *Inorg. Chem.*, 1973, **12**, 2770-2778.

